MD-22 | 243

MILITARY TECHNICAL COLLEGE
CAIRO - EGYPT

# The Use of a Lazer Aided-Interferometer for the Study of the Temperature Field in the Wake of a Cylinder

Tharwat M. Sallam* and Mahmoud H.M.Seliman*

ABSTRACT

Formation, development and instability of the vortices system are observed visually by means of Mach-Zehnder interferometer. A lazer source is used for the optical image of the formed vortices in a variable temperature field.

The investigation is conducted for a group of two-dimensional circular models at a constant Strouhal number of 5000. The excellent agreement, exhibited by the results provided by the observed cases; give an accurate and full description for the evaluation of the flow structure behined the cylinder.

It is concluded that the influence of the temperature field is to retard the evolution of the near-wake, as well as moving the location of the separated shear layers dowstream.

The observed region by the lazer aided-interferometer reveals a good estimation of the bulk flow temperature field behined the cylinder.

## INTRODUCTION

Many investigation have been carried out for flows around a heated cylinder, either at a high flow speed, which present a case of forced convection, or for flow at a case of purely natural convection process [1] and [2] . Very few investigation are concerned with an intermediate case in which forced convection and natural convection occure simultaneously at a low speed of flow passing a hot cylinder surface [3] . Due to the changes in the flow conditions which accompany the changes in density at a low Reynolds number, the fluid characteristics in the shear layer become unstable and exhibit waves with increasing amplitude in the down stream direction, roll up into vortices and finally break down [4] and [5] . The separated region itself has unsteady fluctuating character caused by the existing vortices which periodically carried away with the main flow.

In the scope of the present paper, the investigation of a steady, horizontal, two-dimensional, laminar flow passed a high surface temperature of a cylinder submerged in a normal position to the flow direction is investigated [6] and [7] .

* Lecturer, Faculty of Engineering, Alexandria University, Egypt.

## EXPERIMENTAL ARRANGEMENTS

Figure 1, presents the experimental arrangement. Two test hollow copper cylinders are used 14.5 mm and 9.5 mm in diameter with an equal length of 150 mm. The wind tunnel is provided with a nozzle of contraction ratio 20:1. The experimented cylinder surface is heated by the annular path of a constant water temperature through the constant water tank. Both sides of the cylinder are insulated and the wall temperature is measured by a thermo-couple through the inner surface of its wall. A lazer beam is used as a light source. Photographs are taken on films ASA 400 with a manual camera. The frequancy of the temperature fluctuations is recorded by 8 mm automatic camera with an interval of 10 vortices generation. Time is recorded by the use of stop watch.

## COMPUTATIONS

The numerical computations of the fundemental flow equations are delivered. Navier-Stokes equation continuity equation and energy equation are solved for two-dimensional flow [8] . The density distribution is considered only in the buoyancy term. Effects of the variation in viscosity and thermal diffusion are neglected [9] . The flow field temperature is computed as a function of time, as will as the flow vorticity and stream function [10] . The equation of motion, when the gravitational force is acted only, in Y direction

$$dp_g = -\rho g\, dy = -\rho_\infty g\, dy + g\beta (T - T_\infty)\rho_\infty\, dy \qquad (1)$$

The differential form (Polar coordinates);

$$\frac{\partial v_r}{\partial t} + v_r \frac{\partial v_r}{\partial r} + \frac{1}{r} v_\theta \frac{\partial v_r}{\partial \theta} - \frac{v_\theta^2}{r} = -\frac{1}{\rho}\frac{\partial P^*}{\partial r} + \left(\frac{\partial^2 v_r}{\partial r^2} + \frac{1}{r}\frac{\partial v_r}{\partial r} + \frac{1}{r^2}\frac{\partial^2 v}{\partial \theta^2} - \frac{2}{r^2}\frac{\partial v_\theta}{\partial \theta} - \frac{v_r}{r^2}\right) + g\beta \sin\theta (T - T_\infty) \qquad (2)$$

$$\frac{\partial v_\theta}{\partial t} + v_r \frac{\partial v_\theta}{\partial r} + \frac{1}{r} v_\theta \frac{\partial v_\theta}{\partial \theta} + \frac{v_r v_\theta}{r} = -\frac{1}{\rho}\frac{1}{r}\frac{\partial P^*}{\partial \theta} + \left(\frac{\partial^2 v_\theta}{\partial r^2} + \frac{1}{r}\frac{\partial v_\theta}{\partial r} + \frac{1}{r^2}\frac{\partial^2 v_\theta}{\partial \theta^2} + \frac{2}{r^2}\frac{\partial v_r}{\partial \theta} - \frac{v_\theta}{r^2}\right) + g\cos\theta (T - T_\infty) \qquad (3)$$

Vorticity

$$\varphi = \frac{\partial v_\theta}{\partial r} - \frac{1}{r}\frac{\partial v_r}{\partial \theta} + \frac{1}{r} v_\theta \qquad (4)$$

$$\varphi = -\nabla^2 \cdot \psi \qquad (5)$$

The non-dimensional forms of and are ;

$$\frac{\partial \varphi^*}{\partial t^*} - \frac{1}{r^*}\left(\frac{\partial \psi^*}{\partial r^*}\cdot\frac{\partial \varphi^*}{\partial \theta} - \frac{\partial \psi}{\partial \theta}\cdot\frac{\partial \varphi}{\partial r^*}\right) = \frac{G_r}{2 R_e^2}\left(\cos\theta \cdot \frac{\partial T^*}{\partial r^*} - \frac{\sin\theta}{r^*}\cdot\frac{\partial T}{\partial \theta}^*\right) + \frac{2}{R_e}\cdot\nabla^2_*\cdot\varphi^* \qquad (6)$$

Where; $$\nabla_* = \frac{\partial}{\partial r_*^2} + \frac{1}{r^*}\frac{\partial}{\partial r^*} + \frac{1}{r^{2*}}\frac{\partial^2}{\partial \theta^2} \quad (7)$$

$$\frac{\partial T^*}{\partial t} - \frac{1}{r^*}\left(\frac{\partial \psi^*}{\partial r^*}\cdot\frac{\partial T^*}{\partial \theta} - \frac{\partial \psi^*}{\partial \theta}\frac{\partial T^*}{\partial r^*}\right) = \frac{2}{P_r \cdot R_e}\cdot \nabla^2{}_*\, T^* \quad (8)$$

Boundary conditions;

$$r = r_c \; ; \; \psi = 0 \; , \; \partial\psi/\partial r = 0 \; , \; T = T_w \quad (9)$$

$$r \to \infty \; ; \psi \to r.\sin\theta \; , \; \zeta = 0 \; , \; T \to T_\infty \quad (10)$$

Substituting the boundary conditions, therefore the equation of motion;

$$E^2\frac{\partial \zeta}{\partial t} - \frac{\partial \psi}{\partial \xi}\cdot\frac{\partial \zeta}{\partial \eta} + \frac{\partial \psi}{\partial \eta}\cdot\frac{\partial \zeta}{\partial \xi} = \frac{2}{R}\nabla^2\rho + \frac{E}{2}\cdot\frac{G_r}{R_e^2}\left(\cos\pi\eta\frac{\partial T}{\partial \xi} - \sin\pi\eta\frac{\partial T}{\partial \eta}\right) \quad (11)$$

Where; $E = \pi r \; , \; r = e^{\pi\xi} \qquad \eta = \frac{\theta}{\pi}$

The final finite form of eq. 11 ;

$$\frac{2E}{\Delta t}\left(T_{i,j}^{n+1} - T_{i,j}^{n+\frac{1}{2}}\right) + \frac{1}{4h^2}\left(\psi_{i+1,j}^{n} - \psi_{i-1,j}^{n}\right)\left(T_{i,j+1}^{n+1} - T_{i,j-1}^{n+1}\right) - \frac{1}{4h^2}\left(\psi_{i,j+1}^{n} - \psi_{i,j-1}^{n}\right)\left(T_{i+1,j}^{n+\frac{1}{2}} - T_{i-1,j}^{n+\frac{1}{2}}\right)$$

$$= \frac{2}{P_r \cdot R_e \cdot h^2}\left(T_{i+1,j}^{n+\frac{1}{2}} - 2T_{i,j}^{n+\frac{1}{2}} + T_{i-1,j}^{n+\frac{1}{2}}\right) + \left(T_{i,j+1}^{n+1} - 2T_{i,j}^{n+1} + T_{i,j-1}^{n+1}\right) \quad (12)$$

$$E^2\zeta = -\nabla^2.\psi \quad (13)$$

Equations 12 and 13, are calculated numerically for the stream function, temperature and viscosity by the use of alternating direction implicit scheme (A.D.I) and successive over relaxation technique (S.O.R). Figure 2, presents a typical case of a symmetrical flow, both the stream function and vorticity at Re = 80 .

## RESULTS AND DISCUSSION

Figure 3, shows the flow pattern for a flow passed a hot cylinder surface at Re = 120 and at different iteration time. Figure 4, shows the isotherms around a heated cylinder subjected to air-

stream normal to its axis at different flow conditions. A temperature difference of 14-53 $^{0}$C between the flow and the cylinder surface, which is observed is proved to keep a steady temperature flow field in a range of Reynolds number between 30-100. Increasing the Reynolds number, the temperature pattern grows up to a fluctuated unsteady pattern. Figures 5 and 6, present an unsteady flow pattern case. Figure 7, shows a comparison between the experimental results and its corresponding data attained by Roshko, which reveals a good agreement between both results. Figure 8, shows the flow temperature field through the visualized isotherms around a heated cylinder. The assumptions of the calculation for a constant flow viscosity and density, which is considered only in the buoyancy term, affect the stability of the flow field. However, the buoyant force disturbance changes the Reynolds number limit at which the vortices separate alternately from the cylinder surface. Figures 9 and 10, are the numerical results for a very similar case of the visualized one of Fig. 8. The visualized temperature fringes of Fig. 8, are in a good agreement with the numerical results of Fig. 10.

## CONCLUSION

1. The Use of the lazer aided-interferometer has revealed excellent records which present the overall flow behaviour.
2. The formation, development and instability of the vortices system are observed visually.
3. The visualized cases give a good evaluation for the flow structure behined the cylinder.
4. The numerically computed models are in a fair agreement with the visualized cases.

## REFERENCES

1. T.M. Sallam, et al., 91 st. Annl. Mt. Ohio State Univ., Apr., (1981), U.S.A.
2. T.M. Sallam, et al., Intr. Symp. on Flow Visualization, Bochum, Sept., (1980), W. Germany.
3. Kawaguti, M., J. Phys., Soc. Japan, 8-6 (1953), P. 747.
4. Son, J.S. and Hanraty, T.J., J. of Fluid Mech., 35-2 (1969), P. 369.
5. K.M. Krall, Ph.D. Thesis, University of Minnesota, (1969).
6. T.M. Sallam, Intr. Symp. on Marine Engng., Tokyo, Oct., (1983), Japan.
7. T.M. Sallam, et al., Proc. of MESJ, Oct., (1980), Japan.
8. Wilkie, D. and Fischer, S.A., Proc. Inst. of Mech. Engng., (1964), P. 461.
9. T.M. Sallam. et al., Intr. Symp. on Flow Visualization, Ann Arbor, Mich., Sept., (1983), U.S.A.
10. T.M. Sallam, Intr. Symp. on Combustion, (expected), Mich., Aug., (1984) , U.S.A.

6

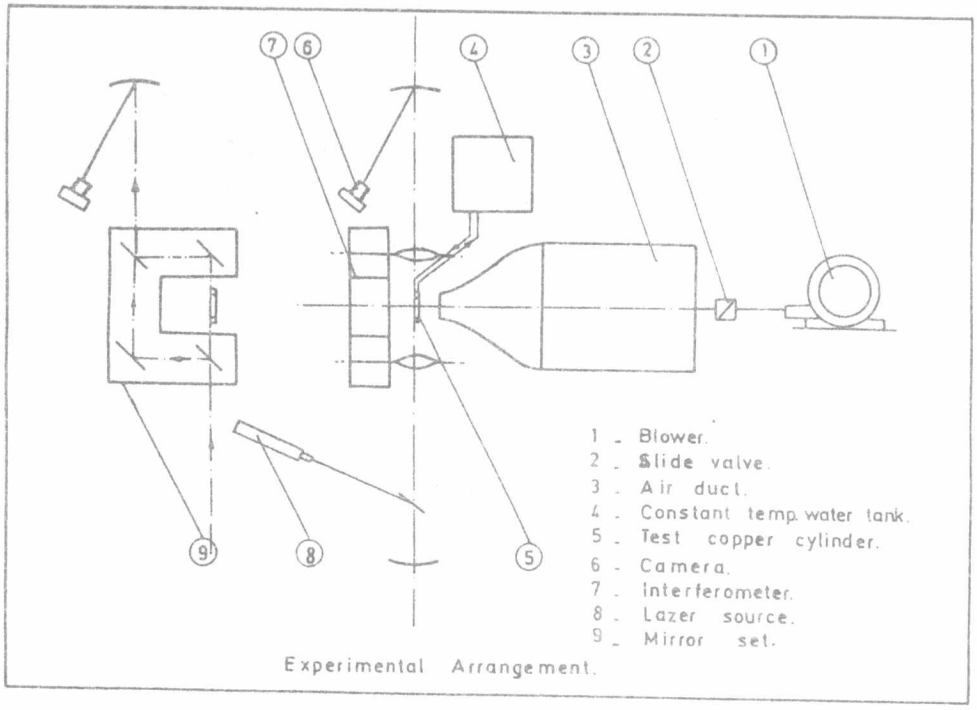


Fig. 1 .

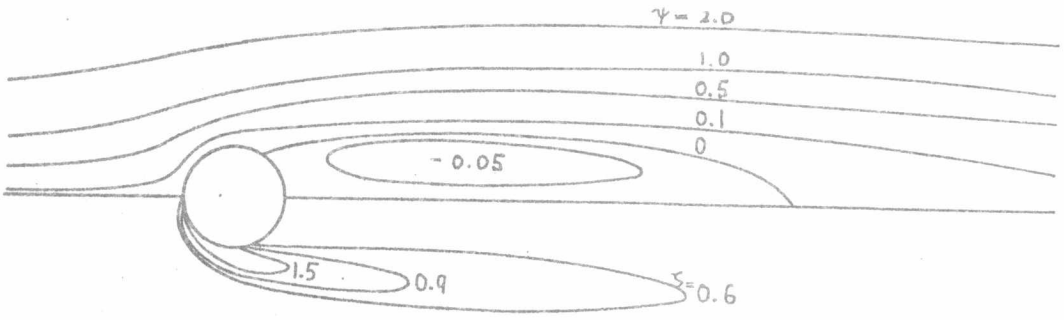


Fig. 2 Flow Pattern & Vorticity $R_e = 80$

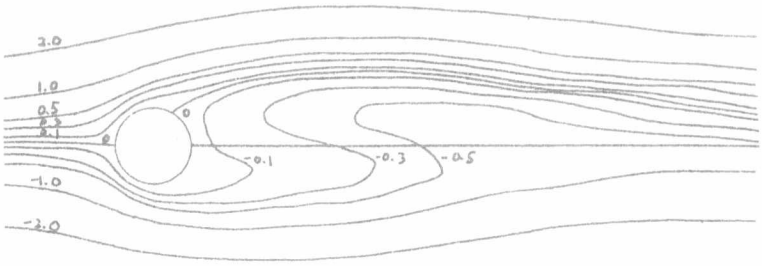


$R_e = 120 \qquad t = 4$

Fig. 3 Flow Patterns

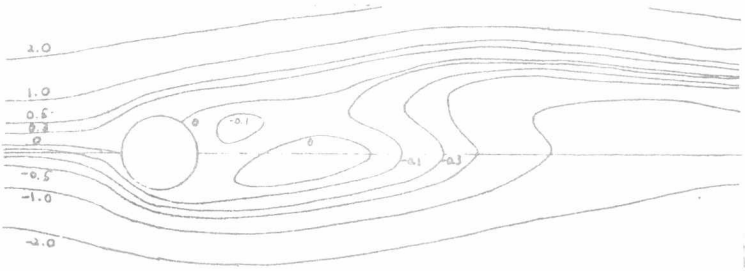


$R_e = 120 \qquad t = 10$

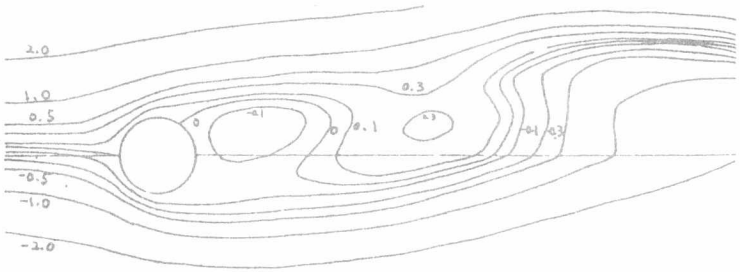


$R_e = 120 \qquad t = 14$

Fig. 4 Isotherms Around a Cylinder

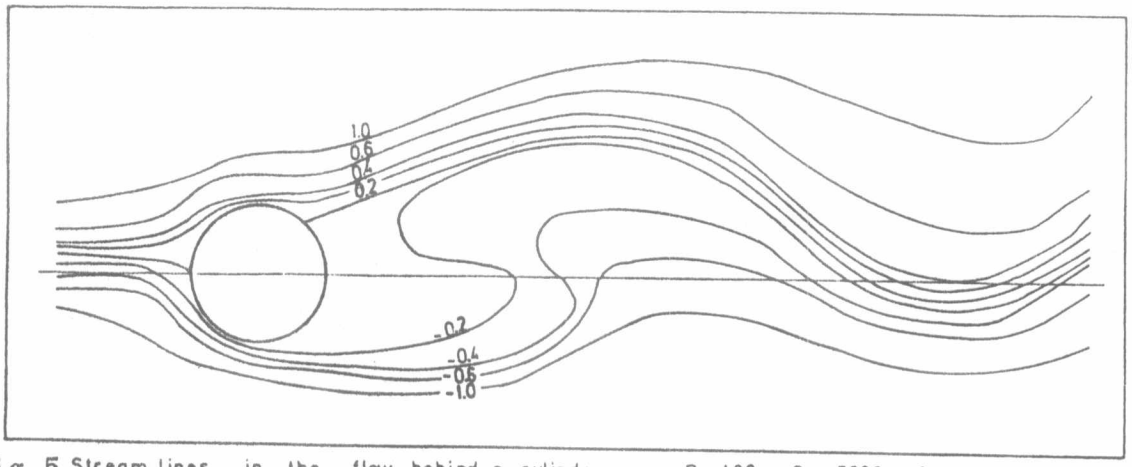


Fig. 5 Stream lines in the flow behind a cylinder $R_e = 100$, $G_r = 5000$ & $t = 19.25$.

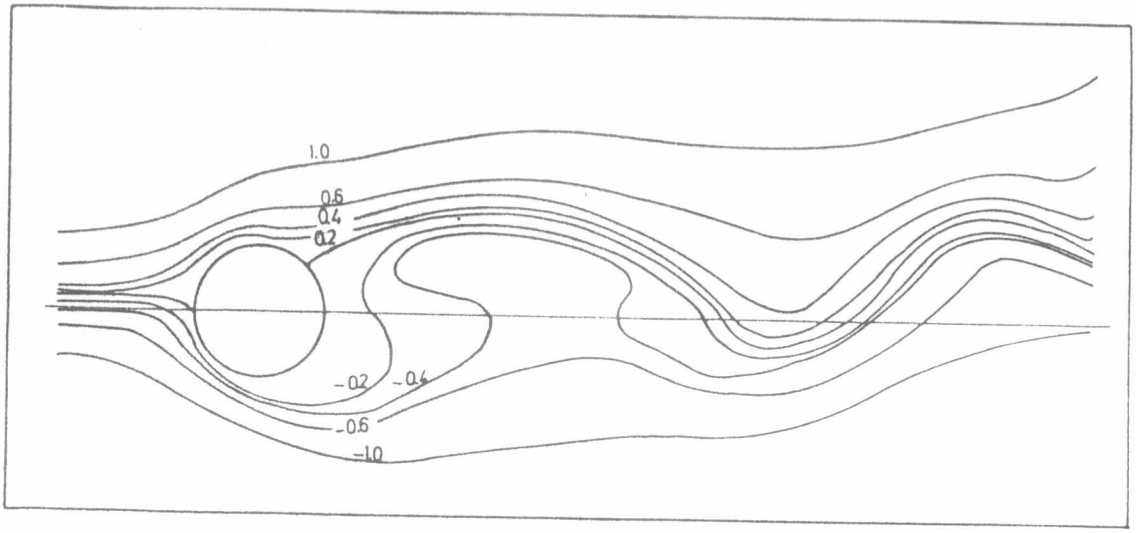


Fig. 6 Stream lines in the flow behind a cylinder $R_e = 100$, $G_r = 5000$ & $t = 13.50$.

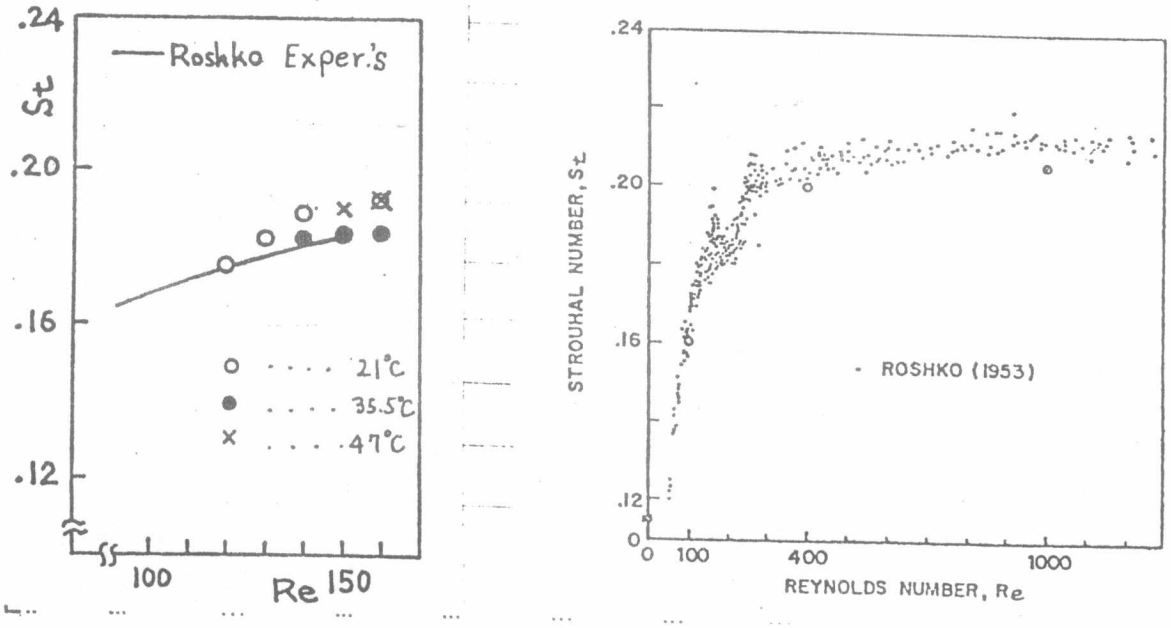


Fig. 7

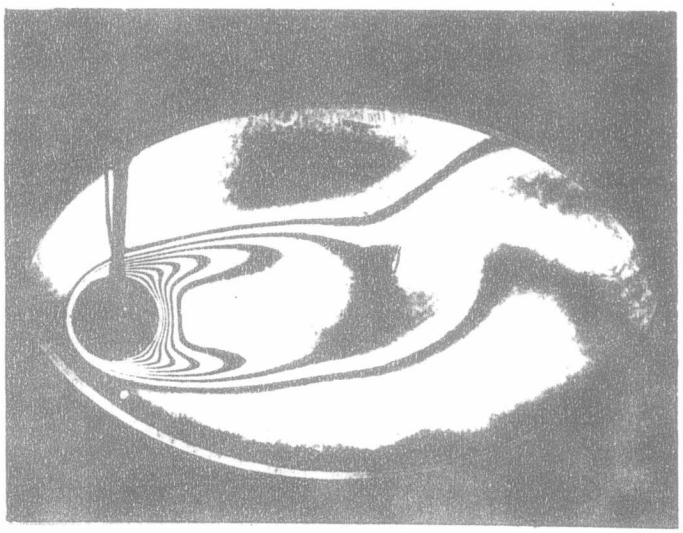

Fig. 8 Flow Around a Cylinder $R_e$ = 100 & T = 35 $^{o}$C

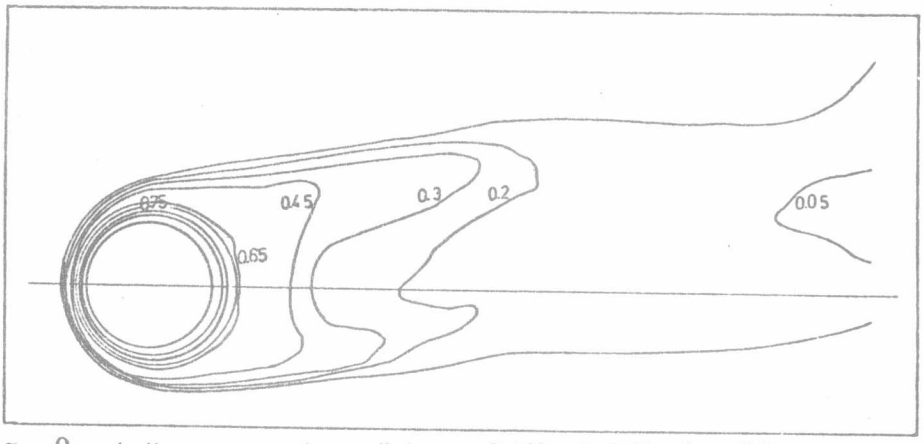


Fig. 9 Isotherms around a cylinder $R_e$=100 , $G_r$= 5000 & t = 19.25.

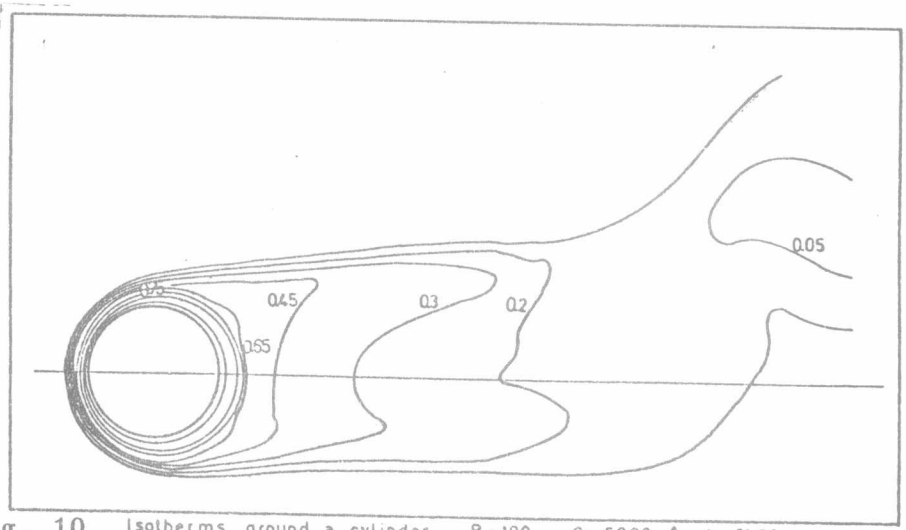


Fig. 10 Isotherms around a cylinder $R_e$= 100 $G_r$= 5000 & t = 31.50.